Discrimination between *Pseudogymnoascus destructans*, other Dermatophytes of Cave-dwelling Bats, and related innocuous Keratinophilic Fungi based on Electronic-nose/GC Signatures of VOC-Metabolites produced in Culture

Alphus Dan Wilson
Forest Insect and Disease Research
USDA Forest Service, Southern Hardwoods Laboratory
Stoneville, MS, USA
e-mail: dwilson02@fs.fed.us

Lisa Beth Forse
Center for Bottomland Hardwoods Research
USDA Forest Service, Southern Hardwoods Laboratory
Stoneville, MS, USA
e-mail: lfwilson@fs.fed.us

Abstract— **White-nose syndrome (WNS), caused by the fungal dermatophyte (*Pseudogymnoascus destructans*), is considered the most important disease affecting hibernating bats in North America. The identification of dermatophytic fungi, isolated from the skins of cave-dwelling bat species, is necessary to distinguish pathogenic (disease-causing) microbes from those that are innocuous. This distinction is an essential step for disease diagnoses, early detection of the presence of microbial pathogens prior to symptom development, and for discrimination between microbes that are present on the skins of hibernating bats. Early detection of *P. destructans* infections of bats prior to symptom development is essential to provide effective early treatments of WNS-diseased bats which significantly improves their chances of survival and recovery. Current diagnostic methods using quantitative polymerase chain reaction (qPCR) for the detection of the microbes on bats require invasive methods (skin swabs) that tend to arouse hibernating bats resulting in consumption of valuable fat reserves that reduce their chances of winter survival. Also, qPCR only indicates the presence and quantity of fungal inoculum on bat skin, but does not indicate that the fungus has infected the host or that a state of disease exists since substrate fungal DNA used for PCR comes from outside of the host (on the surface of the skin) rather than from within the host (in deep subdermal layers of the skin). Consequently, we are developing non-invasive methods for the early detection of WNS-disease and other microbes of bats based on their production of unique mixtures of volatile organic metabolites that may be detected using a dual-technology, electronic-nose/gas chromatography device for identifying and discriminating between the microbial metabolites produced in pure cultures. We determined that the Heracles II e-nose system was effective in discriminating keratinophilic fungal species using principal component analysis (PCA) of smellprints signatures coupled with discrimination index (DI) and gas chromatographic retention times (RTs) of major VOC GC-peaks produced in culture headspace.**

Keywords-electronic aroma detection; e-nose; fungal metabolites; volatile organic compounds; white-nose syndrome.

I. INTRODUCTION

A large diversity of microbes have been isolated from the skins of cave-dwelling bats [1][2]. The skin-swabbing of small mammalian trogloxenes (animals that are temporary cave residents and move freely in and out of caves), particularly insectivorous bats while in hibernation (i.e., in a state of torpor), is a common practice among animal pathologists and wildlife researchers interested in obtaining cultures and conducting diagnostic tests for determining the etiology of various dermatophytic diseases acquired by volant mammals. Bats are known to be attacked by relatively few fungal dermatophytes including *Pseudogymnoascus destructans* (Pd), causing deep-seated skin infections, and *Trichophyton redellii* (ringworm) that causes superficial skin infections [3]. Over the past decade, White-nose Syndrome (WNS), caused by the psychrophilic dermatophyte and pervasive fungal pathogen *P. destructans*, has emerged as the most important disease of cave-dwelling bats in North America, causing extensive mortality and regional population declines of hibernating bat species in the eastern, mid-western and southern United States as well as southeastern Canadian provinces [4]. WNS is known to significantly affect at least eight species of bats in North America including the big brown bat (*Eptesicus fuscus*), the gray bat (*Myotis grisescens*), the eastern small-footed bat (*M. leibii*), the little brown bat (*M. lucifugus*), the northern long-eared bat (*M. septentrionalis*), the Indiana bat (*M. sodalis*), the tricolored bat (*Perimyotis subflavus*), and the southeastern bat (*M. austroriparius*) [5]-[7]. The capability of clinical diagnosticians to detect and discriminate between the microbes growing on the skins of bats is a critical necessity for studying and identifying dermatophytic microbes involved in the complex interactions that occur on bat skins between fungal pathogens, innocuous microbes, and host defense responses that ultimately influence the final outcome of pathogenesis and disease development. To address this diagnostic capability, we are developing new noninvasive diagnostic tools and technologies to identify and discriminate between microbes that grow and multiply on the skins of bats in hibernation and outside of hibernacula.

Electronic-nose (e-nose) devices have been used extensively to identify microbial pathogens in culture which are causal agents of diseases in plants, animals, and humans [8][9]. Various types of e-nose devices, utilizing different operational mechanisms for chemical detection, are particularly useful and effective diagnostic tools for the discrimination of complex gaseous mixtures of volatile

 ISBN: 978-1-61208-581-4

organic compounds (VOCs) that compose the most common metabolic products of microbes released into the headspace of microbial cultures [10][11]. Some important potential advantages of e-nose devices as diagnostic tools, particularly for hibernating bats, are noninvasive early detection of infectious diseases and causal agents (minimal disruption of bat torpor patterns and behavioral disturbances during hibernation), rapid real-time disease detection capabilities using portable e-nose devices, low-cost diagnostic testing, high precision of measurements, low incidence of false positive results, and complex VOC-mixture detections without identifying individual chemical species within diagnostic samples [12][13].

Soil-borne psychrophilic (cold-loving) fungi related to the Pd-pathogen include other *Pseudogymnoascus* species (such as *P. appendiculatus*, *P. roseus*, and *P. verrucosus*), and numerous *Geomyces* species. *Geomyces pannorum* var. *pannorum* is a nonaggressive pathogen that occasionally causes superficial human dermatophytic diseases [14][15]. Although these fungi are somewhat related genetically and metabolically, differences in specific metabolic pathways used by these microbes result in the production of different types, combinations and mixtures of VOCs produced and released into the headspace of microbial cultures. Consequently, unique complex VOC-mixtures, released into culture headspace, may be used as a basis for discriminating between microbial species when analyzed by specialized gas sensor arrays such as e-nose devices [8].

The objectives of this study were to 1) determine the capability of the Heracles II fast gas chromatograph (GC)/E-nose combination-technology instrument to discriminate between related keratinophilic fungi, including both pathogenic and innocuous species, isolated either from bat skin or from soils, a common reservoir of inoculum for fungal dermatophytes of bats, 2) document differences in gas chromatogram component peaks and patterns of VOC fungal metabolite mixtures released into the culture headspace of microbes tested, and 3) develop an aroma map indicating the relatedness and differences in fungal headspace VOC-metabolites of keratinophilic fungi based on 3-dimensional principal component analysis (PCA). The results from this study will be used to evaluate the efficacy of this dual-technology e-nose for discrimination of cultures of *P. destructans* and related fungi.

This paper is composed of an introduction to dermatophytic fungi of bats and the use of e-nose VOC-metabolite detection approaches in section 1, followed by experimental methods used for this work in section 2, describing the specific details of methods used in association with e-nose and GC runs and analytical procedures, followed by experimental results in section 3 providing details of research results and findings for e-nose analyses of fungal VOC metabolites from the headspace of microbial cultures, including sensor output responses to VOCs, PCA e-nose aroma maps of fungal dermatophytes, and associated data. Discussion and conclusions, based on the e-nose experimental results, are presented in section 4 to summarize the significance of findings and new discoveries resulting from this research.

II. MATERIALS AND METHODS

A. Fungal Strains and Growth Conditions

Eight genetically-related keratinophilic fungi were tested in this study including: *Pseudogymnoascus destructans* 20631-21 (PD6), the ATCC type strain originally isolated from a little brown bat (*Myotis lucifugus*) at Williams Hotel Mine, New York; *Pseudogymnoascus destructans* M-3902 (PD3) from West Virginia; *Pseudogymnoascus appendiculatus* UAMH-10509 (PA1) and *Pseudogymnoascus verrucosus* UAMH-10579 (PV1), both isolated from a *Sphagnum fuscum-Picea mariana* bog near Alberta, Canada; *Pseudogymnoascus roseus* 722101 (PR1), the type strain of the genus [16]; *Geomyces pannorum* CCF-340 (GP2), *Geomyces pannorum* CCF-338 (GP5), and *Geomyces pannorum* var. *pannorum* CMF-2582 (GP8) were obtained from the Center for Forest Mycology Research (CFMR; Madison, WI). All media were sterilized at 121°C under 15 PSI for 20 minutes. For long-term storage at −80°C, strains were grown and maintained in 24 hour darkness on Sabouraud dextrose agar (SDA) (4% dextrose, 1% Neopeptone, 2% agar), incubated at 14°C for 8 weeks. Asexual spores were collected by washing sporulating SDA cultures with 5 ml of 0.1% deoctylsulfosuccinate (DSS) in SD broth to which an equal volume of 50% glycerol was added to suspend hydrophobic conidia [17].

B. Sample Preparation and Prerun Procedures

All fungal strains tested were grown on SDA slants in 100 mL Kimax GL45 glass bottles with 40 mL SDA culture medium per bottle. Five glass-bottle cultures were prepared as replications for each strain. Three bottles of uninoculated SDA slants (SAB) served as controls. GL45 PBT open-top screw caps were fitted with Pyrex PTFE-faced silicone rubber septa. Agar slants were inoculated with 20 µl of frozen conidial spore suspension, spread with a sterile glass rod. Cultures were grown in darkness at 14°C for 4 weeks. To allow headspace VOCs to accumulate, cultures were moved to room temperature at 21°C in the dark for 18 hours prior to analysis on a weekly basis. The total quantity of VOCs accumulating in culture headspace over each weekly period were largely removed from bottle cultures for analysis each week so that the quantity of VOCs analyzed weekly indicated the quantity that had accumulated only over a one-week period.

C. Instrument Configuration and Run Parameters

The Heracles II GC/Electronic-nose system (Alpha MOS, Toulouse, France), composed of a dual-column (DB-5 and DB-1701 output) fast-gas chromatograph (GC) with flame-ionization detector (FID) and multiple e-nose sensors, was utilized for all culture VOC-headspace analyses. Fungal VOC-metabolites were manually injected using 15 ml of culture headspace per sample via 20 cc (Cadence Science Inc., Cranston, RI) glass syringe, trapped at 30 °C for 50 s before split-injection at 10 ml/min into DB-5 and DB-1701 GC columns following isothermal heating at 240 °C for 30 s

 ISBN: 978-1-61208-581-4

at 57 kPa of pressure. Analyses were conducted at an initial oven temperature of 50 °C, ramping at 1 °C/s up to 80 °C, then accelerating the heating rate to 3 °C/s up to 250 °C for 21 s. Analyzer injection volume was set at 5000 µl at a speed of 125 µl/s, injection temperature of 200 °C at 10 kPa pressure, injection time 45 s, and venting at 30 ml/min. The two FID detector temperatures, for separate dual columns, were set at 260 °C. Retention times (RTs) of VOCs were recorded for each peak for both GC columns.

The e-nose analyzer component of the dual-technology Heracles II system utilizes a very large number of proprietary sensors in the sensor array. For data analyses involving statistical discrimination algorithms, only those sensors in the array that provided the largest output responses that added significantly to sample discriminations were utilized in data analyses, such as for PCA plots and derivations of aroma signatures or smellprint patterns that define the unique aroma fingerprints of VOC-metabolite mixtures contained within fungal headspace volatiles.

D. Data Acquisition Parameters and Run Schedule

Data acquisition rates for both GC data recording and e-nose data from the sensor array were collected every 0.01 s intervals (100 data points per second) set at a constant data-recording rate for the entire duration of each analysis run. Total run time for all analysis runs was 110 s. Both dual GC-columns and e-nose sensor arrays were purged with ultrapure air or blank samples between each sample analysis.

E. Principal Component Analysis

Three-dimensional principal component analysis (PCA) was performed on e-nose data using Heracles II software to compare the relatedness between aroma signature patterns derived from e-nose sensor array output responses to fungal VOC-metabolite mixtures in culture headspace. Distances between centers of data clusters (PCA mapping distance), derived from sensor array outputs of each fungal culture headspace (aroma classes or sample type), were determined on a PCA plot or aroma map by pairwise comparisons of aroma classes (sample types) in all possible combinations along with aroma Pattern Discrimination Index (PDI), expressed as a percentage, indicating the statistical level of discrimination (P-values) between each corresponding sample type compared based on aroma signature patterns (smellprints).

III. RESULTS

A. Gas Chromatography VOC Peak Analyses

Analyses of gaseous VOC-mixtures produced by individual fungi in culture headspace, based on gas chromatographic (GC) patterns on chromatograms, provided indications of differences in the types and quantities of volatile metabolites produced. Most of the fungi tested produced common metabolites with peaks at RTs of 16.50 s and 26.57 s in 3-week old cultures, although *P. destructans* strains did not produce the 26.57 peak until several months later in older cultures (Table I).

TABLE I. GAS CHROMATOGRAPHY PEAK RETENTION TIMES AND HEIGHTS FOR INDIVIDUAL FUNGAL VOCS PRESENT IN COMPLEX METABOLITE MIXTURES PRODUCED IN CULTURE HEADSPACE

		Peak height[a]				
		Peak RTs of VOCs				
Fungal species	**Strain**	**15.30**	**16.50**	**26.57**	**59.60**	**63.10**
P. appendiculatus	PA1	—	10,680	2,558	—	—
P. roseus	PR1	—	45,507	2,609	—	—
P. verrucosus	PV1	—	29,756	2,628	—	—
G. pannorum	GP2	—	7,361	2,650	—	—
G. pannorum	GP5	—	7,553	3,110	—	—
G. pannorum var. pannorum	GP8	5,542	12,438	—	3,467	—
P. destructans	PD3	—	81,246	PL	—	1,739
P. destructans	PD6	—	42,718	PL	—	1,981

a. Peak heights indicate relative heights of individual peaks, representing separate VOC-metabolites produced by each fungal strain at the indicated RTs (for DB-5 column) derived from GC-chromatographs in separate analyses of headspace from fungal cultures on SDA medium. Symbols PL = VOC peak was produced later (in older cultures).

The VOC-metabolite produced at RT=16.50 varied considerably in peak height for different fungi (up to 11-fold difference in quantities between *G. pannorum* and *P. destructans* strains, but variations in peak heights for the VOC-metabolite produced at RT=26.57 was quite consistent for all fungi tested with the exception of the *G. pannorum* var. *pannorum* strain that did not produce this metabolite. The unique production of two distinct metabolites at RT=15.30 and RT=59.60 only by the *G. pannorum* var. *pannorum* strain was considerably different from the other fungi, particularly *G. pannorum* strains that did not produce these particular VOC-metabolites at all. The two strains of *P. destructans* also produced a unique metabolite at RT=63.10 that was not produced by the other fungi.

B. E-nose Signature Patterns of Headspace Volatiles

Comparisons of differences in e-nose smellprint patterns, derived from multisensor e-nose array outputs of the Heracles II GC/Electronic-nose instrument, provided additional data for discriminating between fungal species based on differences in e-nose multisensor responses to unique VOC-metabolite mixtures produced in culture headspaces. The e-nose smellprints produced by the multisensor array in response to differences in VOC-metabolite mixtures were significantly different from that of SDA-medium alone that served as a control for comparisons to indicate the smellprint of background VOCs released from the common SDA culture medium itself (Figure 1, A-G).

 ISBN: 978-1-61208-581-4

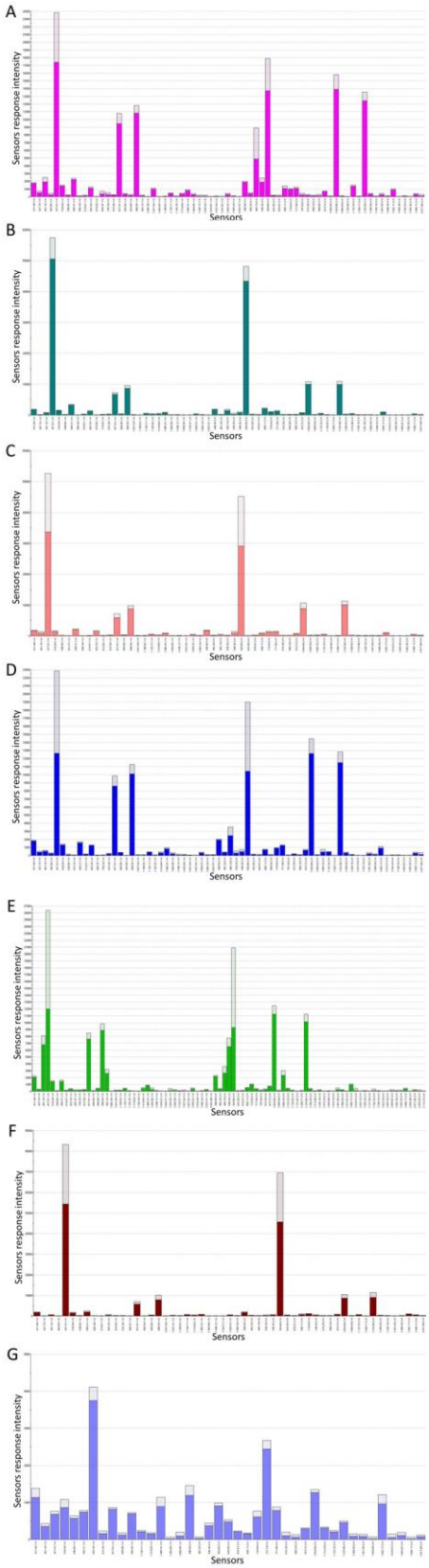

Figure 1. E-nose aroma signature patterns (smellprints) of complex headspace volatile mixtures, composed of fungal VOC metabolites from cultures of fungal dermatophytes and control: A) *P. appendiculatus*, B) *P. roseus*, C) *P. verrucosus*, D) *G. pannorum*, E) *G. pannorum* var. *pannorum*, F) *P. destructans*, and G) SDA medium control.

The sensor numbers, labeled on the x-axis, are listed in the same order for all sample types analyzed. All of the smellprints, produced as sensor responses to VOC headspace volatiles of fungi in culture, varied considerably in sensor response intensity, shown on the y-axis, and in overall smellprints compared with each other and with the SDA-control (Figure 1G). The smellprint pattern of *P. appendiculatus* differed quite drastically from the other *Pseudogymnoascus* species, including the WNS fungal pathogen (*P. destructans*), *P. roseus*, and *P. verrucosus* (Figure 1 A-C,F). The smellprint pattern of *P. appendiculatus* only superficially resembled that of *G. pannorum* strains, but differences in individual sensor intensity responses varied considerably (Figure 1 A,D).

The aroma signature patterns (smellprints) of culture headspace volatile metabolite mixtures of *P. roseus* and *P. verrucosus* were fairly closely related in appearance (Figure 1 B,C). However, the smellprint patterns of *G. pannorum* strains and the *G. pannorum* var. *pannorum* strain GP8 unexpectedly showed very little resemblance (relatively few sensor responses in common), but a very significant number of major and minor sensor responses were considerably different between these two sample types for the majority of sensors responding to VOC-metabolites within the e-nose sensor array (Figure 1 D,E). The smellprint pattern of *P. destructans* strains was uniquely different from those of other *Pseudogymnoascus* species and *Geomyces* species tested with relatively few major sensor responses and many minor sensor responses at low intensities (Figure 1 F).

C. Principal Component Analysis

The differences observed in sensor responses of the Heracles II e-nose sensor array to complex gaseous mixtures of volatile metabolites released into culture headspace were analyzed statistically using principal component analysis (PCA) to measure and quantify the differences between e-nose aroma signatures produced by individual fungi. Pairwise comparisons of e-nose aroma profiles, tested in all possible combinations to assess and measure these differences, indicated widely varying PCA mapping distances (between data clusters for individual fungal species) and statistical differences as measured using a percentage Pattern Discrimination Index (PDI) for each pairwise comparison (Table II). These analyses collectively included 36 distinct PCA-pairwise comparisons between individual strains of each fungal species and between the fungal strains and uninoculated SDA slant (SAB) controls.

All nine fungal strains tested showed high levels of significant differences from SDA-culture medium controls, both in terms of PCA mapping distances (range of 21,992-106,723 mapping units) and percentage PDI (range of 72.3-98.7%). PDI results provided precise numerical values (percentage indications) of differences between sample types in all possible combinations. The higher the value, the lower the relatedness between each paired combination.

 ISBN: 978-1-61208-581-4

TABLE II. PAIRWISE-COMPARISONS BETWEEN E-NOSE AROMA PROFILES OF CULTURE HEADSPACE VOC-METABOLITES OF FUNGAL DERMATOPHYTES AND SABOURAUD DEXTROSE AGAR CONTROL BASED ON 3-D PCA

Aroma class 1	Aroma class 2	PCA mapping distance[a]	PDI (%)[b]
PA1	PR1	43,728.52	91.98
	PV1	9,466.80	22.49
	GP2	16,164.98	64.55
	GP5	14,123.66	58.11
	GP8	21,517.88	76.88
	PD3	82,334.10	84.94
	PD6	28,688.58	46.70
	SAB	33,558.06	88.32
PR1	PV1	42,352.60	88.24
	GP2	58,469.24	97.89
	GP5	55,983.53	97.69
	GP8	62,777.83	98.26
	PD3	38,967.67	57.28
	PD6	17,424.10	25.88
	SAB	68,801.81	98.71
PV1	GP2	16,861.30	56.84
	GP5	14,904.61	50.69
	GP8	22,026.64	69.63
	PD3	81,088.75	83.76
	PD6	25,798.87	39.68
	SAB	29,460.40	78.39
GP2	GP5	4,006.78	24.00
	GP8	10,541.13	70.59
	PD3	97,246.99	89.50
	PD6	42,247.27	67.83
	SAB	22,116.79	93.74
GP5	GP8	12,396.70	76.75
	PD3	94,709.95	88.99
	PD6	40,020.94	65.42
	SAB	24,683.17	94.86
GP8	PD3	101,318.45	90.28
	PD6	46,643.56	72.09
	SAB	21,992.46	94.65
PD3	PD6	55,673.80	61.93
	SAB	106,723.11	89.36
PD6	SAB	51,724.00	72.25

a. PCA aroma mapping distances indicate actual plotting distances between centers of data clusters for each combination of sample types compared. b. Percentage values for aroma Pattern Discrimination Index (DPI) indicate the P-value of significant differences (expressed as a percentage) for each pairwise comparison between sample types being compared, based on PCA-statistical testing of aroma plot data.

The *P. appendiculatus* strain (PA1) PCA-mapping data cluster was most significantly different from *P. roseus* strain (PR1), *G. pannorum* var. *pannorum* strain (GP8), and *P. destructans* strain (PD3) based on mapping distance (between data clusters) and PDI (%). Strain PA1 of *P. appendiculatus* was considerably less different (more related) to *P. verrucosus* strain (PV1), but moderately different from *G. pannorum* strains (GP2 and GP5) as indicated by lower mapping distances and PDI values.

P. roseus strain PR1 showed a PCA mapping data cluster that had very high significant differences in aroma mapping distances and PDI values from strains GP2 and GP5 of *G. pannorum* and strain GP8 of *G. pannorum* var. *pannorum*, but much less differences with data clusters of strains PD3 and PD6 of *P. destructans.*

P. verrucosus strain PV1 displayed PCA mapping data clusters with highly significant differences in aroma mapping distances and PDI values when compared with *P. destructans* strain PD3, but only moderate differences with strains GP2 and GP5 of *G. pannorum*, strain GP8 of *G. pannorum* var. *pannorum*, and lower levels of significant differences with *P. destructans* strain PD6.

The PCA mapping data cluster of *G. pannorum* strain GP2 had low levels of differences in aroma mapping distances and PDI values when compared with data clusters of *G. pannorum* strain GP3, but differences in these two PCA statistical parameters were highly significant when compared with PCA data clusters of *P. destructans* strains PD3 and PD6 as well as *G. pannorum* var. *pannorum* strain GP8. Very similar results were observed for PCA comparisons of the mapping data cluster of *G. pannorum* strain GP5 with *P. destructans* strains PD3 and PD6 and *G. pannorum* var. *pannorum* strain GP8.

Construction of a 3-dimensional plot (aroma map) of all sample types tested using PCA provided a visual means of comparing the PCA mapping distances between data clusters of each sample type as well as an overall Discrimination Index (DI), indicating the relative overall strength or level of discrimination between all sample types included in the PCA test. Displayed DI values are validated by the Heracles II software (using green highlighting), indicating a passing PCA test at $P \leq 0.10$ level of significance when a successful discrimination between sample types is achieved.

The plotted aroma data cluster of *G. pannorum* var. *pannorum* strain GP8 was most obviously separated from the other fungi tested as indicated in the 3-dimensional PCA aroma map of fungal VOC-metabolite mixtures in culture headspace (Figure 2). The overall discrimination index (DI) was 67.0 for this 3-D PCA plot.

A most surprising result was the discovery that G. pannorum var. pannorum strain GP8 produced an aroma signature that was highly different from *G. pannorum* strains GP2 and GP5.

Mapping data clusters in the 3-D PCA plot of e-nose aroma signature data among *Pseudogymnoascus* species generally were well separated with only a few minor overlaps for some combinations between species. Data clusters for *P. destructans* strains were most distant (least related) with *P. appendiculatus* strain PA1, intermediately distant from (moderately related with) *P. verrucosus* strain PV1, and least distant from (most related to) *P. roseus* strain PR1.

 ISBN: 978-1-61208-581-4

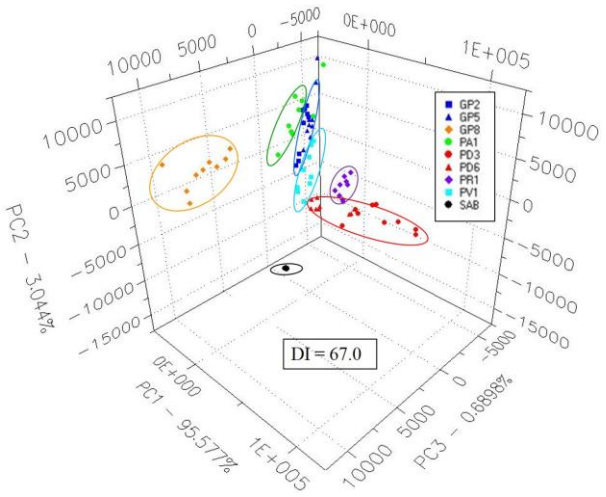

Figure 2. E-nose aroma map showing the chemical relatedness between fungal dermatophytes using Principal Component Analysis (PCA).

The percentages of total variance, accounting for the variability explained by each orthogonal principal component, are as follows: PC 1 = 95.6%; PC 2 = 3.0%; and PC 3 = 0.7%. Thus, most of the variability in the PCA was accounted for by PC 1 (x-axis), whereas PC 2 (y-axis) and PC 3 (z-axis) account for only a small proportion of the total variance.

IV. DISCUSSION AND CONCLUSIONS

Analyses of VOC-peak patterns from GC chromatograms of volatile metabolites produced in culture headspace indicated that most of the fungi tested produced metabolites at the same two RTs, suggesting the production of some common VOCs and the likely use of similar metabolic pathways by these genetically-related fungi. Differences in VOC peak heights at specific RTs provide evidence that different keratinophilic fungal species and strains may utilize slightly different metabolic pathways or have gene duplications within the genome that produce varying quantities of common VOC-metabolites in culture [18].

G. pannorum var. *pannorum* produced two unique VOC-metabolites that were different from those produced by all other related fungal species tested. Significant differences in VOC-metabolite mixtures (produced in culture headspace) in addition to pathogenicity differences, combined with PCA pairwise-comparisons and e-nose mapping data of VOC-metabolite mixtures, all suggest that *G. pannorum* (strains GP2 and GP5) and *G. pannorum* var. *pannorum* strain GP8 function metabolically as separate species and that *G. pannorum* var. *pannorum* perhaps should be elevated as a distinct new *Geomyces* species, rather than just a variety, or perhaps a new *Pseudogymnoascus* species. The taxonomy of *Geomyces* and *Pseudogymnoascus* species currently is in a state of flux and some researchers already consider *G. pannorum* var. *pannorum* to be a *Pseudogymnoascus* species based on more recent DNA-homology results from genetic studies.

The authors chose to compare the relatedness between smellprint patterns, derived from e-nose sensor array output responses to fungal VOC-metabolites, using the PCA method with PDI values because these e-nose analysis procedures are most useful for providing precise numerical values of differences with statistical levels of significance. The WNS-pathogen *P. destructans* was most closely related metabolically to *P. roseus* and *P. verrucosus*, and less related to *P. appendiculatus* based on 3-dimensional PCA mapping distance, PDI, and data clustering on the e-nose aroma map. These results were consistent with similar indications of relative genetic relatedness between these species based on genetic analyses using genomic DNA-homology tests [19]. The uniquely different mixtures of VOC-metabolites produced in culture headspace by strains of *P. destructans*, compared to its non-pathogenic cave-dwelling psychrophilic (cold-loving) and saprophytic relatives consisting of other *Pseudogymnoascus* and *Geomyces* species commonly in cave sediments, indicate that the Pd-pathogen has shifted its metabolic pathways toward pathogenic phenotypes and greater utilization of keratinogenic substrates. Recent evidence suggests that this shift in substrate specialization from saprobic to pathogenic phenotypes in *P. destructans* has occurred at the expense of reduced saprotrophic enzyme activity [20]. This data suggests that *P. destructans* has co-evolved over time with its bat hosts and moved away from the utilization of carbon sources in the environment, leading to its somewhat reduced capacity for saprotrophic growth. Although *P. destructans* is still considered a competent saprotroph that persists and sporulates in cave sediments (presumably due to its emergence from non-pathogenic ancestors), its reduced activity of urease and endoglucanase saprobic enzymes provide evidence that it may be shifting toward increasingly pathogenic activity [20][21].

Our results indicate that the Heracles II GC/e-nose dual-technology instrument was effective in discriminating between genetically-related species of *Pseudogymnoascus* and *Geomyces*, common keratinophilic fungi of bat skin, based on the production of unique VOC-metabolite mixtures in culture headspace. Furthermore, PCA provided indications of differences in metabolic relatedness between fungal species based on unique mixtures of fungal VOC-metabolites produced. This capability of e-nose devices to detect and discriminate between complex VOC-metabolites produced by pathogenic and non-pathogenic keratinophilic fungi of bats could potentially provide a new effective means for the noninvasive early detection and diagnosis of devastating wildlife diseases, such as WNS. A cheaper, more portable e-nose device potentially could be useful for both rapid diagnosis of the disease in living bats and for determining the cause of death post-mortem [22][23]. The WNS-epizootic has already killed over six million hibernating bats in North American since the disease was first detected and identified in New York State in 2006 [1][24][25]. Consequently, there is a need for a rapid, noninvasive method for early WNS disease detection at the geographical advancing front of the epizootic in order to allow for the application of very early,

 ISBN: 978-1-61208-581-4

more effective WNS-control applications, particularly prior to the appearance of WNS-disease symptoms, as newly approved treatments are developed and become available.

ACKNOWLEDGMENT

The authors thank Charisse Oberle for assistance in running Heracles II GC fast-gas/e-nose analyses of headspace volatiles from fungal cultures.

REFERENCES

[1] K. J. Vanderwolf, D. F. McAlpine, D. Malloch, and G. J. Forbes, "Ectomycota associated with hibernating bats in eastern Canadian caves prior to the emergence of White-nose Syndrome," Northeastern Naturalist, 2013, 20, pp 115–130, doi: 10.1656/045.020.0109.

[2] L. J. A. N. Johnson, et al., "Psychrophilic and psychrotolerant fungi on bats and the presence of *Geomyces* spp. on bat wings prior to the arrival of white nose syndrome," App Environ Microbiol, 2013, 78, pp 5465–5471, doi:10.1128/ AEM.01429-13

[3] J. M. Lorch, et al., "The fungus *Trichophyton redellii* sp. nov. causes skin infections that resemble white-nose syndrome of hibernating bats," J. Wildl. Dis., 2015, 51, pp 36-47.

[4] US Fish and Wildlife Service, "White-nose syndrome map 2017," USFWS, Hadley, Massachusetts, [Online]. Available from: whitenosesyndrome.org/resources/map. Accessed May 2017.

[5] D. S. Blehert, et al., "Bat white-nose syndrome: an emerging fungal pathogen?" Science, 2009, 323, pp 227, doi:10.1126/science.1163874.

[6] G. R. Turner and D. M. Reeder, "Update of white-nose syndrome in bats," Bat Research News, 2009, 50, pp 47–53.

[7] F. Courtin, W. B. Stone, G. Risatti, K. Gilbert, and H. J. Van Kruiningen, "Pathologic findings and liver elements in hibernating bats with white-nose syndrome," Vet. Pathol., 2010, 47, pp 214–219, doi:10.1177/0300985809358614.

[8] A. D. Wilson, D. G. Lester, and C. S. Oberle, "Development of conductive polymer analysis for the rapid detection and identification of phytopathogenic microbes," Phytopathology, 2004, 94, pp 419–431.

[9] A. D. Wilson and M. Baietto, "Advances in electronic nose technologies developed for biomedical applications," Sensors, 2011, 11, pp 1105-1176.

[10] A. D. Wilson, and M. Baietto, "Applications and advances in electronic-nose technologies," Sensors, 2009, 9, pp 5099-5148.

[11] A. D. Wilson, "Diverse applications of electronic-nose technologies in agriculture and forestry," Sensors, 2013, 13, pp 2295–2348.

[12] A. D. Wilson, "Advances in electronic-nose technologies for the detection of volatile biomarker metabolites in the human breath," Metabolites, 2015, 5, pp 140-163.

[13] A. D. Wilson, "Recent progress in the design and clinical development of electronic nose technologies," Nanobiosensors in Disease Diagnosis, 2016, 5, pp 15-27.

[14] C. Gianni, G. Caretta, and C. Romano, "Skin infection due to *Geomyces pannorum* var. *pannorum*," Mycoses, 2003, 46, pp 430–43, doi:10.1046/j.1439-0507.2003.00897.

[15] H. Zelenková, "*Geomyces pannorum* as a possible causative agent of dermatomycosis and onychomycosis in two patients," Acta Dermatovenerol Croat, 2006, 14, pp 21–25.

[16] R. S. Currah, "Taxonomy of the Onygenales: *Arthrodermataceae*, *Gymnoascaceae*, *Myxotrichaceae* and *Onygenaceae*," Mycotaxon, 1985, 24, 1–216.

[17] H. T. Reynolds and H. A. Barton, "Comparison of the white-nose syndrome agent *Pseudogymnoascus destructans* to cave-dwelling relatives suggests reduced saprotrophic enzyme activity," PLoS ONE, 2014, 9, e86437.

[18] H. T. Reynolds, H. A. Barton, and J. C. Slot, "Phylogenomic analysis supports a recent change in nitrate assimilation in the white-nose syndrome pathogen, *Pseudogymnoascus destructans*," Fungal Ecology, 2016, 23, pp 20-29.

[19] A. M. Minnis and D. L. Lindner, "Phylogenetic evaluation of *Geomyces* and allies reveals no close relatives of *Pseudomgymnoascus destructans*, comb. nov., in bat hibernacula of Eastern North America," Fungal Biology, 2013, 117, pp 638-649.

[20] H. T. Reynolds and H. A. Barton, "Comparison of the white-nose syndrome agent *Pseudogymnoascus destructans* to cave-dwelling relatives suggests reduced saprotrophic enzyme activity," PLoS ONE, 2014, 9, e86437.

[21] H. T. Reynolds, T. Ingersoll, and H. A. Barton, "Modeling the environmental growth of *Pseudogymnoascus destructans* and its impact on the white-nose syndrome epidemic," J. Wildl. Dis., 2015, 51, pp 318-331.

[22] A. D. Wilson, "Biomarker metabolite signatures pave the way for electronic-nose applications in early clinical disease diagnoses," Current Metabolomics, 2017, 5, pp 90-101.

[23] A. D. Wilson, "Electronic-nose applications in forensic science and for analysis of volatile biomarkers in the human breath," Journal of Forensic Science and Criminology, 2014, 1(S103), pp 1-21.

[24] A. Gargas, M. T. Trest, M. Christensen, T. J. Volk, and D. S. Blehart, "*Geomyces destructans* sp. nov. associated with bat white-nose syndrome," Mycotaxon, 2009, 108, pp 147-154.

[25] J. M. Lorch, et al., "Experimental infection of bats with *Geomyces destructans* causes white-nose syndrome," Nature, 2011, 480, pp 376-378.

 ISBN: 978-1-61208-581-4